Expert Systems with Applications, Volume 184, December 2021, Article number 115504
DOI:10.1016/j.eswa.2021.115504

Fault simulations and diagnostics for a Boeing 747 Auxiliary Power Unit

Christos Skliros
Integrated Vehicle Health Management Centre, School of Aerospace, Transport and Manufacturing, Cranfield University, Bedfordshire, MK43 0AL, United Kingdom
e-mail: C.Skliros@cranfield.ac.uk

Fakhre Ali
Integrated Vehicle Health Management Centre, School of Aerospace, Transport and Manufacturing, Cranfield University, Bedfordshire, MK43 0AL, United Kingdom
e-mail: f.ali@cranfield.ac.uk

Ian Jennions
Integrated Vehicle Health Management Centre, School of Aerospace, Transport and Manufacturing, Cranfield University, Bedfordshire, MK43 0AL, United Kingdom
e-mail: i.jennions@cranfield.ac.uk

Highlights

- Auxiliary Power Unit (APU) fault simulations.
- Sensitivity assessment of component faults on the APU performance.
- Diagnosis of single and multiple APU component faults.
- Identification of the strengths and weaknesses of system-level diagnostics.

Keywords

Condition-Based Maintenance, Auxiliary Power Unit, Fault simulations, Diagnostics

Abstract

Health monitoring of aircraft systems is of great interest to aircraft manufacturers and operators because it minimises the aircraft downtime (due to avoiding unscheduled maintenance), which in turn reduces the operating costs. The work that is presented in this paper explores, for a Boeing 747 APU, fault simulation and diagnostics for single and multiple component faults. Data that corresponds to healthy and faulty conditions is generated by a calibrated simulation model, and a set of performance parameters (symptom vector) are selected to characterise the components health state. For each component under examination, a classification algorithm is used to identify its health state (healthy or faulty) and the training strategy that is used considers the existence of multiple faults in the system. The proposed diagnostic technique is tested against single and multiple fault cases and shows good results for the compressor, turbine, Load Control Valve (LCV) and Fuel Metering Valve (FMV), even though these faults present similar fault patterns. On the contrary, the classifiers for the Speed Sensor (SS) and the generator do not provide reliable predictions. As regards the SS, the sensitivity assessment for this component showed that the existence of faults in the other components can sometimes mask the SS fault. The reason that the generator diagnosis fails under the proposed diagnostic technique is attributed to the fact that it has only a very slight influence on the other symptom vector parameters. In both cases, additional diagnostic strategies are suggested.

Published by Elsevier. This is the Author Accepted Manuscript issued with: Creative Commons Attribution Non-Commercial No Derivatives License (CC:BY:NC:ND 4.0).
The final published version (version of record) is available online at DOI:10.1016/j.eswa.2021.115504. Please refer to any applicable publisher terms of use.

1. Introduction

1.1. Auxiliary Power Unit - System Background

The Auxiliary Power Unit (APU) is a system installed in all commercial aircraft and its purpose is to provide bleed air and electrical power to the aircraft systems. The APU is mainly operated when the aircraft is at the airport gate, when the main engines have not started, or in case of an emergency during flight. The APU is one of the main drivers of maintenance as reported by Liu et al. [1], and APU maintenance costs significantly increase due to component faults that lead to unscheduled maintenance, as reported by Yabsley et al. [2]. Hence this system is worthy of study.

The APU consists of a single spool gas turbine engine that transfers energy to an electrical generator through its shaft. Bleed air is extracted either from the gas turbine's compressor or from an independent compressor (load compressor) connected to the main shaft. Representative examples for these configurations are provided by Skliros et al. [3] and by Siebel et al. [4]. The gas turbine bearings are lubricated and protected from overheating by a lubrication and cooling system. An electric motor and an ignition system are used to start the APU. Fuel flow during starting and steady-state is regulated by the fuel system, which is controlled by the APU control unit, and in modern APUs, this is a Full Authority Digital Electronic Controller (FADEC).

Previously [3] an APU simulation has been developed, calibrated, and validated against Boeing 747 APU test data. This was previous work by the current authors, which explored electrical power and bleed air extraction across a number of healthy test cases. This paper aims to take this rich simulation and extend it into a simulation of fault modes, for which experimental testing cannot readily be performed, against which to test a diagnostic technique that is able to identify multiple component faults.

1.2. Literature Review on APU Health Monitoring Methods

The APU has been identified by aircraft operators as a major driver for maintenance as reported by Liu et al. [1]. The system's complexity and the fact that APU performance data is rarely available, make health monitoring of the APU a very challenging task. Based on the available information and the scope of the work conducted, researchers use either model-based or data-driven methods to investigate the system's health state.

In model-based methods, performance data generated by a simulation model is compared with real systems data and, based on this comparison, component faults can be identified. These methods require accurate information regarding the component design characteristics. However, this information belongs to the system manufacturer and it is not generally available in public domain literature. For this reason, model-based methods are not used frequently. The two most important model-based health monitoring studies have been reported by Gorinevsky et al. [5] and Gorinevsky et al. [6]. Both studies follow a similar approach in which a physics-based simulation model calculates the values of the performance parameters for given boundary conditions under healthy and faulty states. The model differences between the healthy and degraded conditions are used as an input to a fault estimator module, which has been designed to identify component faults. The results reported demonstrate that the proposed methods can identify fault modes to an acceptable level, considering the uncertainties and noise that exist in real systems.

Since model-based methods are not easily produced, and detailed engineering knowledge is needed, most published research efforts use data-driven methods. These methods aim at identifying system faults by analysing data collected from real APU systems. The analysis is conducted by machine

learning algorithms that can detect patterns in the data and correlate them with known fault modes, or by statistical methods that assign probabilities to a component being healthy or faulty. The bibliography for data-driven methods in general is vast, and a comprehensive review of these methods has been provided by Lei et al. [7].

Data-driven methods require the system's performance data under healthy and degraded conditions. This can be either real system's data taken from the aircraft data reporting systems or data generated from a simulation model. In the work conducted by Vianna et al. [8] a physics-based model is used to simulate the system's operation under eight fault modes and the diagnostic analysis that was conducted considered single faults. In this analysis, the differences in the performance parameters between the healthy and degraded conditions were used to train a Classification and Regression Tree. The results demonstrated that the healthy state could be detected in all cases, but some fault modes were misclassified due to insufficient modelling data. Also, Pascoal et al. [9], used a simulation model to generate APU data under three different component faults, and based on the Exhaust Gas Temperature (EGT), bleed air pressure and fuel flow, a linear regression classifier and a neural network classifier were trained to classify healthy and faulty conditions under single fault cases. The results showed that the neural network classifier had higher diagnostic accuracy compared to the linear regression.

Data-driven methods have been used to predict the Remaining Useful Life (RUL) of the APU system or its components. Wang et al. [10] used data from the Aircraft Condition Monitoring System to train a random forest algorithm that predicts the EGT based on other APU performance parameters. The system's health state was baselined by the random forest model and the system's degradation over time is modelled by a Bayesian probabilistic framework which assumes that degradation evolves based on a Dynamic Linear Model (DLM). The DLM is used to predict the system's RUL. This method was tested against field data of APUs belonging to a small fleet of aircraft and presented satisfactory results. Liu et al. [1] also used aircraft data to develop an algorithm that predicts the APU's RUL. Gaussian Process Regression and Relevance Vector Machine are used to predict the RUL. The EGT is used as the major RUL prediction parameter, and the influence of the bleed mass flow and gearbox oil pressure and temperature on RUL predictions are investigated. The main conclusion of this analysis was that the RUL prediction accuracy increases when more prediction parameters were considered.

The common target of all health monitoring approaches is to accurately identify component faults, or predict their RUL, in order to advise prompt maintenance action that can minimize downtime. The health monitoring studies for APU systems, presented in this section, are the most representative examples. However, many diagnostic methods can be applied to an APU depending on the scope of the research and the components examined. In the work conducted by Skliros et al. [11], a review of the different diagnostic methods that can be applied to a complex system such as the APU is presented. The selection of the most appropriate method depends on the subsystems or components under examination, taking into account all the available information.

2. Failure modes selection and diagnostic methodology

2.1. Scope of the work

From a system operator's point of view, a health monitoring analysis is most valuable if it can accurately assess the system's health state and identify the Line Replaceable Units (LRUs) that should be replaced to minimise the system's downtime and avoid unscheduled maintenance. In real systems almost all components have a degree of degradation and, many times, different failure modes have similar fault patterns. This phenomenon makes the identification of the degraded components a

challenging task. The aim of this work is to assess the APU health state and develop a diagnostic technique that is able to identify degraded components for single or multiple fault conditions.

In order to achieve this, a fault mode for each component under investigation is selected and its effects on the system performance is explored by injecting it into the simulation model. The effects that single and multiple faults impose on the system performance are analysed by conducting various runs for single and multiple faults under different fault severity levels. This analysis reveals the different component faults that result in similar fault patterns, and aids in the definition of the component fault severity range that will be used in the diagnostic analysis.

Following that, various simulations for single and multiple component faults are conducted, and a rich database that includes many different fault combinations is produced. Using these datasets, for each component under examination, a classification algorithm is trained appropriately in order to recognise the component health state. The most critical part of the work that is presented in this paper is that the classifier training strategy considers the existence of multiple component faults. Thus, the classifiers are trained to recognise each component health state while other components can be either healthy or faulty. Datasets that include single and multiple component faults, and have been generated independently from the training datasets, are then used to test the diagnostic classifiers. The results of the various test cases reveal the strengths and weaknesses of the proposed technique. In the final part of this paper, methods to enhance the overall diagnostic capability are proposed.

2.2. Failure Modes Selection Methodology

The Boeing Company that supports and funds this project, has identified the most frequent component faults in APU systems. Investigation of these faults by injecting them into the APU rig would be unsafe, therefore an alternate approach is taken. In this work, the validated gas turbine model is modified in order to simulate component faults, for steady-state conditions. The aim of this paper is to explore the effect that different component faults impose on the APU performance and propose a diagnostic technique that can identify the component health state for single and multiple faults, based on the system's performance parameters. The investigation of all possible fault modes that can develop in APU components is not possible due to their excessive number. For this reason, the components that have been reported to fail more frequently were chosen, and for each component a single fault mode was selected based on the relevant studies in the literature.

At this point, it is important to note that the APU which is used as a case study in this paper has an unknown history, and its health state is assumed to be deteriorated compared to a refurbished unit. The component characteristics (e.g. compressor map, turbine map, combustor efficiency, and generator windings resistance) that are used in the simulation model were adjusted in order to match the experimental data as was described in Skliros et al. [3]. These characteristics, which are calibrated against the experimental data, are used as a "healthy" baseline for the analysis that follows.

Starting with the gas turbine subsystem, the components that have been reported to influence the APU performance are the compressor, turbine, and Load Control Valve (LCV). As reported by Kurz and Burn [12], the fault modes that develop in the combustor do not cause a major effect on the gas turbine system thermodynamic performance, and for this reason this component is not included in the analysis.

Faults in the compressor can develop due to a number of different reasons (e.g. fouling, erosion, corrosion, or increased tip clearance). Most of these conditions are generated from the accumulation of foreign objects on the compressor blades which can result in changes in the geometry of the blades,

and finally affect the compressor characteristics. The effects that these faults impose on the compressor performance have been discussed by many researchers and various experimental and simulation studies exist [12]–[14]. The relevant literature suggests that the changes in the compressor performance characteristics (mass flow, pressure ratio and isentropic efficiency) depend on the nature of the fault. For instance, faults that are related with increased tip clearance have been reported to decrease all three compressor performance characteristics, as reported by Graf et al. [15] and Frith [16], while fouling or erosion faults have a much stronger influence on the isentropic efficiency compared to the mass flow and pressure ratio as reported by Mund and Pilidis [17] and Fouflias et al. [18]. The compressor fault that is considered in this paper assumes that the compressor isentropic efficiency has a small decrease (up to 1%) compared to the baseline efficiency, while the relationship between the mass flow and pressure ratio in the performance map remains unaffected compared to the baseline characteristic.

As regards the turbine, the high temperature of the gas flow that enters this component damages the turbine blades and this results in various fault modes (e.g. fouling, erosion, corrosion, increased tip clearance, or thermal distortion). The relevant literature studies report that turbine degradation has a much stronger influence on the isentropic efficiency, compared to the flow capacity, as reported by Boyle [19] and Diakunchak [20]. The turbine fault that is considered in this paper, emulates a condition in which the turbine isentropic efficiency has a small decrease (up to 1%), while the mass flow and pressure ratio characteristics in the performance map do not change compared to the baseline.

The LCV directs the mass flow that exits the compressor to the aircraft pneumatic system. The LCV is a pneumatically operated valve and it consists of many different parts. The part that typically fails is the valve's actuator, and this is usually caused by leakage between the piston chamber of the pneumatic actuator, degraded springs, or excessive piston friction, as reported by Shang and Liu [20], and by Daigle and Goebel [21]. These faults result in deviation of the valve's commanded position, and this affects the bleed flow extraction, which in turn affects the entire APU performance. The LCV fault that is considered in this paper, simulates a sticking valve that reduces the extracted bleed flow compared to the operator's settings. This fault results in operating conditions that correspond to APU operation under lower bleed flow settings.

As regards the control system, a fault mode in the Speed Sensor (SS) is investigated. The SS calculates the APU rotational speed based on the frequency of a gear in the gearbox. Measurement of the gear frequency is achieved by a monopole in the speed sensor that changes the generated magnetic flux based on the gear's rotation. The magnetic flux measurements are converted to electrical signals that correspond to the rotational speed, and these are transferred to the APU controller. Overheating or ageing of the SS electrical parts result in faults in the SS. These faults can be bias, drift, noise, or gain in the output signal, as has been reported by Balaban et al. [23] and Goebel and Yan [24]. The fault mode that is considered in this paper simulates a condition that the output signal has a positive bias compared to the input signal. This means that the rotational speed signal that is transferred to the controller is higher than the real APU rotational speed.

The effects in the APU performance due to a fault in the Fuel Metering Valve (FMV) are also considered. The FMV is a solenoid valve, which regulates the fuel flow to the gas turbine according to the controller commands, thus it can be subjected to both mechanical and electrical faults. As regards the electrical parts, overheating can result in an increase in the resistance of the solenoid windings or, in the worst case, can cause an open circuit in one of the windings. Degradation of the valve's mechanical components and seals can also result in jamming or locked rotating parts as reported by

Balaban et al. [24], Xiao et al. [25] and Cao et al. [26]. Electrical and mechanical faults can result in the following conditions:

- Drift in the valve's position
- Offset in the valve's position,
- A sticking valve at a constant position
- An inoperative valve

The fault mode that is considered in this work simulates a sticking valve condition. This fault results in a constant fuel flow that is increased compared to the healthy state.

Finally, the influence of a generator fault in the APU performance is also explored. The generator is a complex component and it can develop faults that belong to electrical or mechanical parts. The work that is presented in this paper considers only generator faults that belong to electrical parts. Electrical faults are mostly generated from overheating, which results in an increase in resistance of the generator windings. If the resistance increases excessively open circuits can be created in the generator's windings, as it is reported by Batzel et al. [28], Batzel and Swanson [29] and Tantawy et al. [30]. The generator fault that is simulated in this work considers the increase in the generator stator resistance. The increased stator resistance increases the power imposed on the gas turbine shaft, which in turn affects the gas turbine performance.

2.3. Diagnostic Methodology

The proposed diagnostic technique is designed to identify component health state based on system performance parameters. In order to diagnose the component health state, it is necessary to run simulations for all possible fault combinations and identify appropriate fault characteristics. Classification algorithms, if trained appropriately, can identify fault characteristics for complex systems as reported by Bettocchi et al. [31] and Bettocchi et al. [32]. For this reason, under the proposed diagnostic method, for each system component a classification algorithm is trained to recognize its health state (healthy or faulty).

The training strategy that is adopted to train the classifiers considers the simultaneous existence of multiple faults in the system. The diagnostic technique that is proposed in this work is motivated by the work conducted by Hare et al. [33], in which Neural Network (NN) classification algorithms were trained to recognize multiple faults in an aircraft Environmental Control System. The training strategy, that considered multiple component faults, provided more accurate diagnostic predictions compared to the training strategy that was based on the single fault hypothesis.

The diagnostic technique that is discussed in this paper is applied to the APU which is an equally complicated system, by considering more components and expanding the training scenarios compared to those used by Hare et al. [33]. The classification algorithms are trained by considering four scenarios regarding the system's health state (Table 1). This training strategy aims to train each component's classifier to recognize the health state of the component under investigation, while multiple faults exist in the system. The simplest scenario is based on a single fault hypothesis. This scenario assumes that only one component is degraded while all other components are healthy. The second and third scenarios assume that some components in the system can be healthy while others can be degraded. These scenarios replicate realistic maintenance situations, where some components are replaced, while others remain in the system. Finally, the fourth scenario assumes that all components suffer from a degree of degradation due to the system's operation and the individual

component ageing. The advantages and limitations of the proposed method are discussed in Section 5.

Table 1 System health state scenarios

	Scenario 1	Scenario 2	Scenario 3	Scenario 4
Healthy	All components are free from degradation.	One component (different from the component under examination) is degraded and all other components are free from degradation.	The component under examination is free of degradation and other components can be either healthy or faulty.	The component under examination is free of degradation but all other components are degraded.
Faulty	Component under examination is degraded but all other components are free from degradation.	The component under examination and one more component are degraded.	The component under examination is degraded and other components can be either healthy or faulty.	The component under examination is degraded and all other components are degraded.

3. Fault simulations

3.1. Simulation Model Background

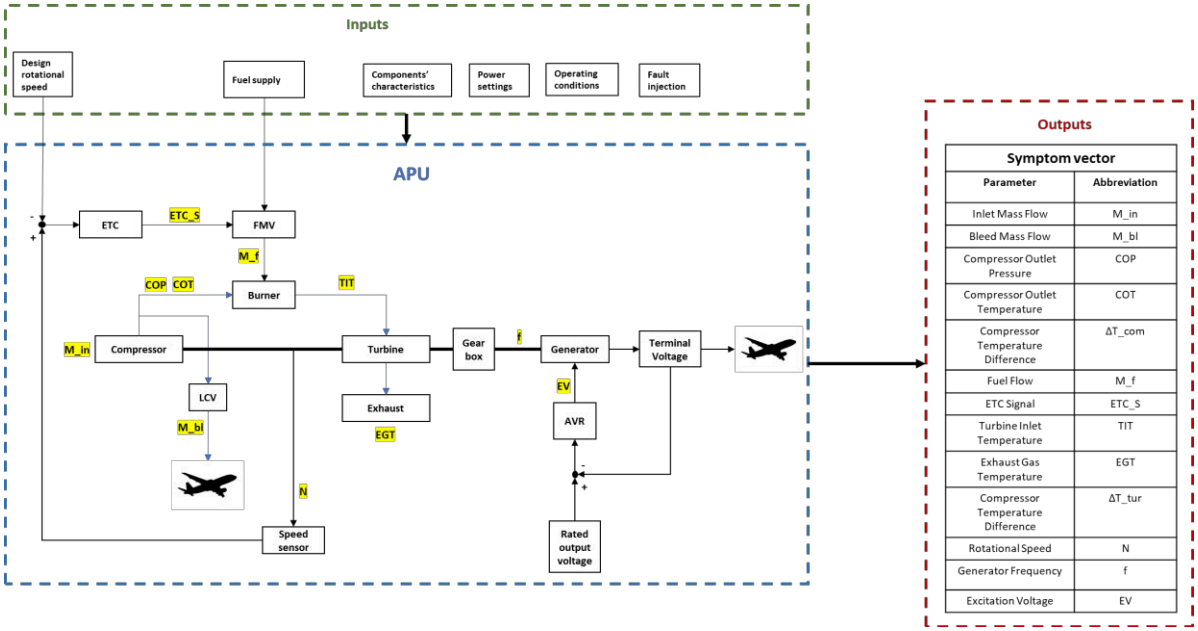


Figure 1 APU model schematic

Figure 1 presents the schematic diagram of the APU model. This model includes a 0-D simulation of the gas turbine, fuel control system and the electric generator. This model has been developed in Simulink by leveraging the Toolbox for Modelling and Analysis of Thermodynamic Systems (T-MATS) library and the characteristics of the components have been calibrated against experimental data from the GTCP660-4 APU. The inputs to the model are the fuel supply, the rated rotational speed, the operating conditions, the component characteristics, the power settings, and the component health state. The model's outputs are the APU performance parameters, from which the symptom vector values are extracted. The symptom vector characterises the system's health state and is created from virtual sensors located across the system (Figure 1). These virtual sensors capture the parameters that represent operation of the components and together form the symptom vector, which is the input to the diagnostic algorithm.

Table 2 presents the failure modes that are considered in this analysis, as a result of the discussion given in Section 2.2. In the rest of this section, the fault injection mechanism of the respective component is presented, and the degradation range that will be considered for each one of them is be explained. The classification algorithm that is selected for each component is discussed in Section 5.

Table 2 Components faults that are considered into the diagnostic analysis

Subsystem	Symbol	Component	Simulated failure mode and degradation range	Classification algorithm
Gas turbine	N1	Compressor	Decreased efficiency up to 1%.	Logistic regression
	N2	Turbine	Decreased efficiency up to 1%.	Logistic regression
	N3	Load Control Valve	Bleed flow reduced up to 1%.	Support vector machine
Control	N4	Speed sensor	Output signal increased up to 0.5%.	Classification tree
Fuel	N5	Fuel Metering Valve	The valve is stuck in a position that is increased up to 1% compared to the healthy case.	Classification tree
Generator	N6	Generator	Generator's stator resistance increased up to 5%.	k-nearest neighbour

3.2. Gas Turbine

The gas turbine's model schematic is presented in Figure 1 and the iterative solver that calculates the model's solution is presented in Figure 2. The iterative solver aims to drive E1-E3 to zero by changing the values of the Independent Variables. The gas turbine's performance parameters are based on the inlet mass flow, and the operating points on the compressor and turbine maps. They are calculated by thermodynamic equations included in T-MATS.

The literature that is cited in Section 2, and investigates faults in the compressor and turbine, reports various fault modes that result in changes in the mass flow, pressure ratio and efficiency of the compressor or turbine. In this work, a simplified approach for these component faults is taken by assuming that the compressor or turbine isentropic efficiency decreases, while the characteristics of the mass flow and the pressure ratio, as they are defined in the component design maps, remain unaffected. The compressor and turbine isentropic efficiencies are defined by the following equations:

$$\eta_{com,isen} = \frac{\Delta T_{com}}{\Delta T_{com,isen}} = \frac{COT - CIT}{COT_{(isen)} - CIT} \quad (1)$$

$$\eta_{tur,isen} = \frac{\Delta T_{tur}}{\Delta T_{tur,isen}} = \frac{TIT - EGT}{TIT - EGT_{(isen)}} \quad (2)$$

The reduced efficiency of the compressor and turbine change the component operating point, and this affects the entire system's performance. The effects that these faults impose on the symptom vector are discussed in Section 4.1.

The fault mode considered in the LCV simulates a condition that the valve is stuck, and it cannot provide the requested bleed flow. This fault mode is emulated by decreasing the bleed flow demand and the system's performance corresponds to healthy operation under lower power settings. The changes imposed on the symptom vector due to these faults are further elaborated in Section 4.1.

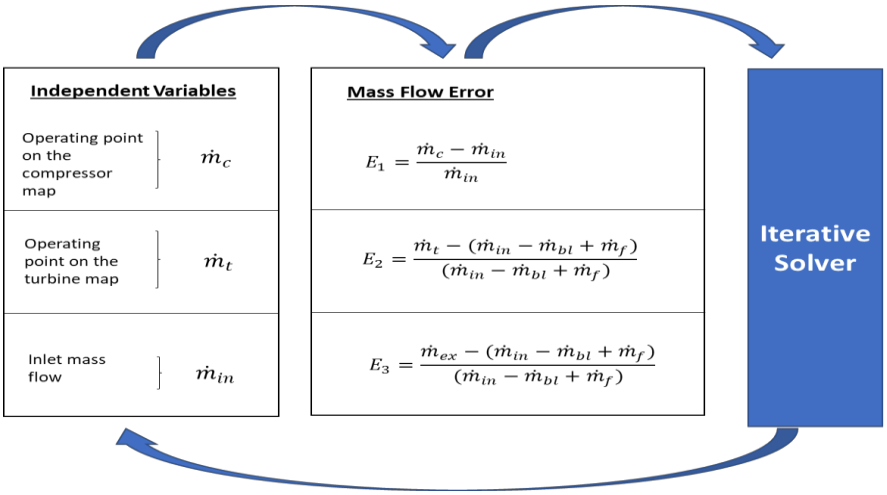


Figure 2 Gas turbine solver schematic

3.3. Control and Fuel System

The APU's control system monitors the machine's performance and ensures its safe operation. The part of the control system discussed in this paper is related to the adjustment of fuel flow to the gas turbine. The components that are involved with fuel control are illustrated in Figure 1.

The fuel flow to the gas turbine is adjusted in order to maintain constant rotational speed regardless of the changes in power settings, operating conditions, or the degradation of the components. The fuel flow is regulated by the FMV which is controlled by the APU Electronic Turbine Controller (ETC). The ETC is simulated by a PI controller that accepts as an input the difference between the sensed rotational speed and the rated rotational speed, regulating the FMV's position between fully open and fully closed.

The maximum fuel flow to the gas turbine (FMV fully open) is given by the APU maintenance manuals and based on this information the controller's signal is regulated accordingly.

The fault injected in the FMV assumes that the valve is stuck and the fuel flow to the gas turbine is constant regardless of the controller's command. The gas turbine's rotational speed is transferred to the controller by a speed sensor (SS). For the purposes of this work, the sensor's dynamic characteristics are ignored. The failure mode that is injected into the SS simulates a condition that the signal transferred to the ETC has a constant positive bias. The changes caused to the symptom vector due to the FMV and SS faults are discussed in Section 4.2.

3.4. Generator

The electric generator is a synchronous machine that consists of an excitation and a load circuit. Mechanical power is transmitted to the generator's shaft from the gas turbine through a gearbox (Figure 1). The generator provides constant output voltage regardless of the load, the changes in the

rotational speed or the generator's health state. This is achieved via an Automatic Voltage Regulator (AVR) that adjusts the excitation voltage in order to regulate the armature's magnetic flux accordingly.

The generator model assumes steady-state operation and balanced load across its phases. The output Line-to-Line voltage is calculated by the following equations:

$$V_{out} = V_{arm} - I_{load} * \left(\sqrt{{X_{in}}^2 + {R_{stat}}^2}\right) \quad (3)$$

$$V_{arm} = \sqrt{2} * \pi * \varphi * \frac{N_{gen}}{20} \quad (4)$$

In Equation 3, V_{arm} is the armature's voltage, I_{load} is the current flow through the electric load, R_{stat} is the stator resistance and X_{in} is the sum of the stator and armature inductive reactance. The stator's resistance is $R_{stat} = 0.4\ \Omega$ and the value of the generator's total inductive reactance (X_{in}) was adjusted in order that the simulation results could match the experimental data. The excitation circuit and the AVR are simulated by a PI controller that compares the output voltage with the rated voltage and adjusts the armature's magnetic flux accordingly. However, as opposed to the excitation voltage, the magnetic flux cannot be measured in real systems. For this reason, an empirical relationship between the magnetic flux and the excitation voltage is created. Experimental data of the excitation voltage are correlated with the simulated armature's magnetic flux through a polynomial equation and the following empirical relationship is established:

$$V_{ex} = 5497.328 * \varphi^2 - 1235{,}807 * \varphi + 73.54 \quad (5)$$

The generator's operation creates a counter torque to the generator shaft, which is transmitted to the gas turbine's shaft. The power demand from the generator is calculated based on the following formula:

$$P_{gen} = \frac{V_{arm}^2}{R_{arm}} \quad (6)$$

In Equation 6, the armature's resistance is: $R_{arm} = 1.52\ \Omega$.

The generator fault mode considered in this work assumes that the stator resistance (R_{stat}) increases due to overheating. The changes imposed on the symptom vector under the generator fault, for various degradation levels, are presented in Section 4.3.

4. Sensitivity assessment of the APU model under the influence of faults

In this section, the component faults are injected into the simulation model, the changes in the APU performance are discussed and the model's sensitivity is assessed by simulating various levels of degradation for each component fault. The sensitivity assessment ensures that the simulation results are consistent with the APU performance under faulty conditions and contributes to the definition of the component degradation ranges that will be investigated in the diagnostic analysis.

The boundary conditions selected to conduct the fault simulations correspond to the maximum power settings imposed on the APU rig that was used to calibrate the model, these are:

- Bleed flow: 3kg/s
- Electric power: 25 kW
- Ambient temperature: 20 °C
- Altitude: Sea level

o Mach number: APU stationary

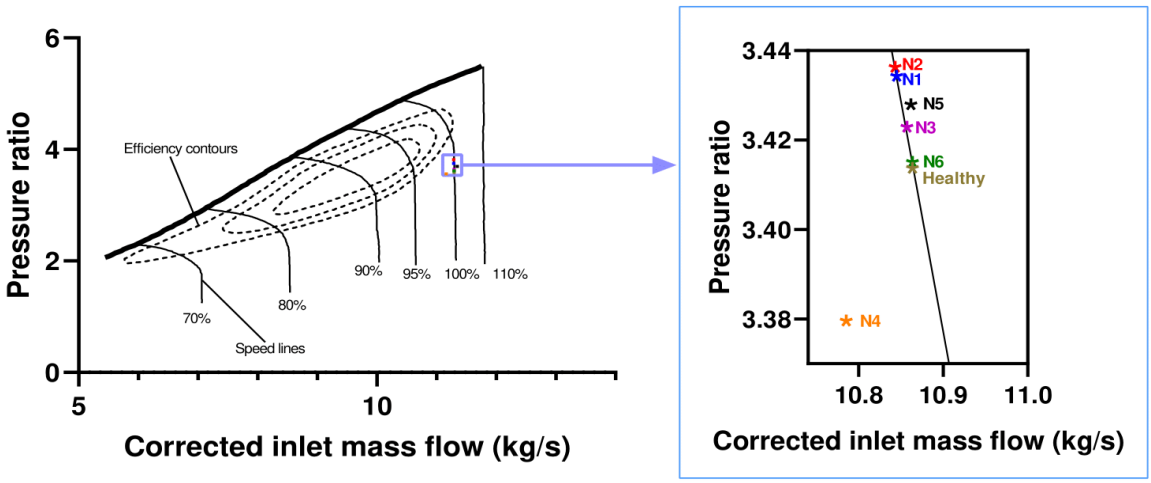


Figure 3 Compressor operating points

The influence of each component fault is investigated in isolation, following the methodology reported by Norton [34]. Also, representative examples of multiple faults that create similar changes in the symptom vector and result in ambiguous fault conditions are discussed in this section. The influence that all fault combinations impose on the symptom vector cannot readily be analysed due to the large number of all possible fault combinations. The effects that multiple faults have on the APU performance are captured by classification algorithms that are used to identify each component's health state under single and multiple faults and are further discussed in the diagnostic analysis in Section 5.

The compressor operating point influences the APU performance under the various faults. For this reason, the operating points that correspond to the faults that are considered in this paper (for a single case) are illustrated in Figure 3. The points N1-N6 correspond to the component faults shown in Table 2. The change of the compressor operating point aids the understanding of the APU performance under faulty conditions and will be discussed throughout this section.

4.1. Gas turbine faults

In this section, the effects of the gas turbine component faults on the APU performance are analysed. Initially, each fault is discussed in isolation and then, at the end of this section, representative examples of multiple faults are presented.

Starting with the compressor, a fault in this component is simulated by reducing the component efficiency and the imposed changes on the symptom vector are presented in Figure 4. In this, and subsequent figures, the deviation of a variable from healthy (y-axis) is plotted for each variable (x-axis). The variables are shown in the table of Figure 1 and represent the main parameters governing the performance of the APU. Each individual deviation is connected with a solid line to give a visual representation of the symptom vector and conveys no other meaning. The change of the compressor's operating point that corresponds to decreased efficiency by 1% is illustrated in Figure 3 (N1). Due to the fact that the APU maintains constant rotational speed, the compressor operating point remains

on the same speed line and the relationship between the inlet mass flow and the pressure ratio is dictated by the shape of the speed line on the compressor map.

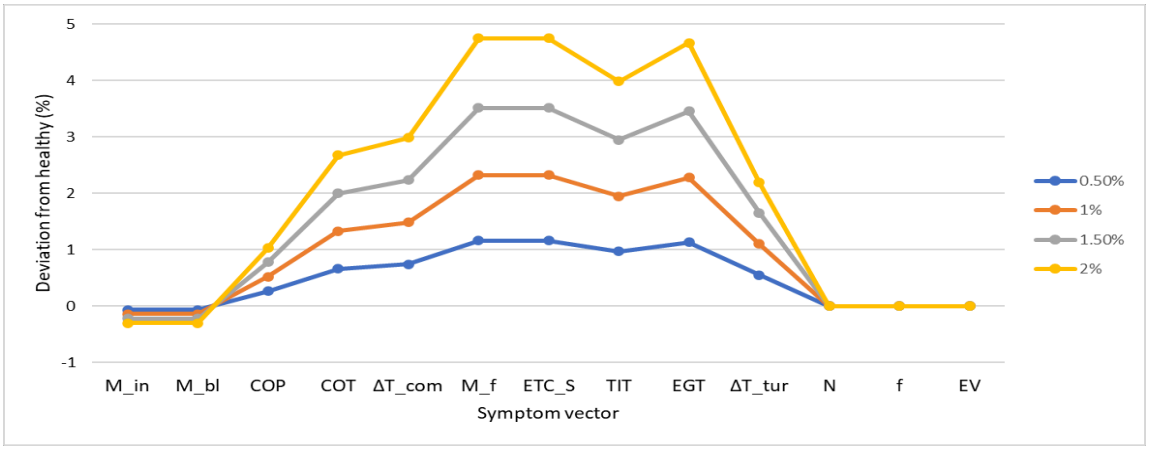


Figure 4 Sensitivity assessment for the compressor fault

Under the discussed compressor fault, the decreased compressor efficiency shifts the compressor operating point to reduced mass flow. As a consequence, based on the compressor's design characteristics (Figure 3), the pressure ratio and the compressor outlet temperature increase. The power consumed by the compressor can be calculated from:

$$P_{com} = \dot{m}_{in} * C_{p,air} * \Delta T_{com} \tag{7}$$

Assuming that the specific heat of air at constant pressure ($C_{p,air}$) remains almost constant, the compressor power depends on two opposing factors: the inlet mass flow and the temperature difference across the compressor. Since the temperature difference across the compressor presents a stronger change compared with the inlet mass flow (Figure 4), the compressor power consumption increases. As a consequence, since the controller keeps the rotational speed constant, the turbine needs to provide more power, which leads to a rise in the fuel flow.

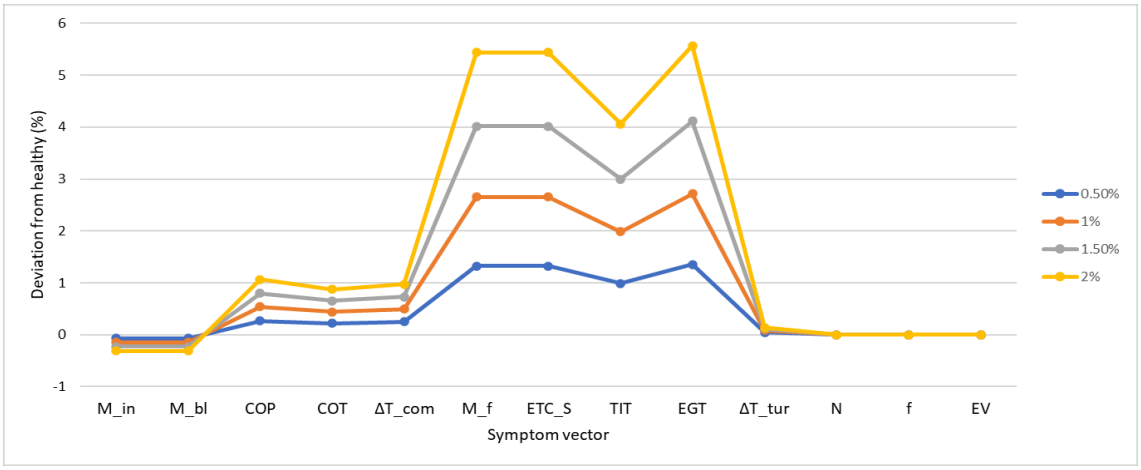


Figure 5 Sensitivity assessment for the turbine fault

The effects of a turbine fault on the APU performance are investigated next. The turbine fault is emulated by decreasing the turbine efficiency and Figure 5 illustrates the changes in the symptom vector due to this fault for 4 severity levels. Figure 3 (N2) presents the change in the compressor operating point due to a decrease in the turbine efficiency by 1%. The reduced turbine efficiency drives

the compressor and turbine operating points to reduced mass flow. Thus, since the APU keeps its rotational speed constant, the COP and COT increase due to the shape of the compressor characteristic line (Figure 3).

The changes in the fuel flow are associated with the power balance between the compressor and the turbine. The power provided by the turbine is calculated by the following equation:

$$P_{tur} = (\dot{m}_{in} + \dot{m}_f - \dot{m}_{bl}) * C_{p,gas} * \Delta T_{tur} \quad (8)$$

Based on the changes in the performance parameters presented in Figure 5, the value of the factor "$(\dot{m}_{in} + \dot{m}_f - \dot{m}_{bl})$" remains almost constant. However, the temperature difference across the turbine reduces since it is calculated by Equation 2, and the turbine efficiency decreases. Thus, under the discussed fault, the power provided by the turbine decreases. As regards the compressor power consumption, it is calculated by Equation 7 and based on the changes in the APU performance parameters in Figure 5, it is observed that the decrease in the inlet mass flow is much lower compared to the increase in the temperature difference across the compressor. Thus, the compressor power consumption, under the turbine fault, increases. The decrease in the power provided by the turbine in combination with the increase in the compressor power consumption creates a tendency of the APU to reduce its rotational speed. However, since the controller is designed to keep the rotational speed constant, the fuel flow increases.

The compressor and turbine are mounted on the same shaft, and for this reason, a fault in one of these components affects the performance of the other, therefore it is worthwhile to compare the changes that the compressor and turbine faults impose on the APU performance. Figure 6 presents the changes in the symptom vector when the efficiency of each component individually is decreased by 1%.

Initially, it is noticed that even though the compressor operating point is almost the same for both faults (Figure 3: N1 and N2), the COT increases more under the compressor fault. This is explained due to the fact that the COT is calculated from Equation 1 and the compressor isentropic efficiency reduces (the Compressor Inlet Temperature (CIT) remains constant).

Another observation that can be extracted by comparing the changes in APU performance under the compressor and turbine faults (Figure 6) is that the TIT is almost the same for both faults, while the EGT presents a stronger increase under the turbine fault compared to the compressor fault. The TIT depends on 2 factors: the COT and the fuel flow. The COT is higher under the compressor fault, while the fuel flow is higher under the turbine fault. The influence of the compressor and turbine faults on these parameters result in almost equal changes in the TIT for both faults. This is associated with the temperature difference across the turbine. The EGT is calculated by Equation 2 and it is based on the TIT and the turbine efficiency. The decreased turbine efficiency under the turbine fault results in a lower temperature difference across the turbine, and this explains the increased EGT observed under the turbine fault compared to the compressor fault.

Finally, it can be observed that even though the compressor and turbine faults have the same fault severity (efficiency decrease by 1%), there is a higher increase in the fuel flow under the turbine fault. The fuel flow ensures that the turbine power matches the compressor power consumption. The compressor and turbine power are calculated by Equation 6 and 7, respectively. By comparing the magnitude of the changes in the inlet mass flow and the COT in Figure 6, it can be concluded that the compressor power consumption increases under both the compressor and the turbine fault. Under the compressor fault, the compressor power consumption increases, and for this reason, the fuel flow increases until the power balance between the compressor and the turbine is achieved. Under the turbine fault, the turbine power decreases (because the turbine efficiency drops) and since the turbine

power must satisfy the compressor power demand, the fuel flow rises. Moreover, as it was described in the previous paragraph, under the turbine fault the compressor power consumption also increases and this results in a further increase of the fuel flow, hence the increased fuel flow under the turbine fault.

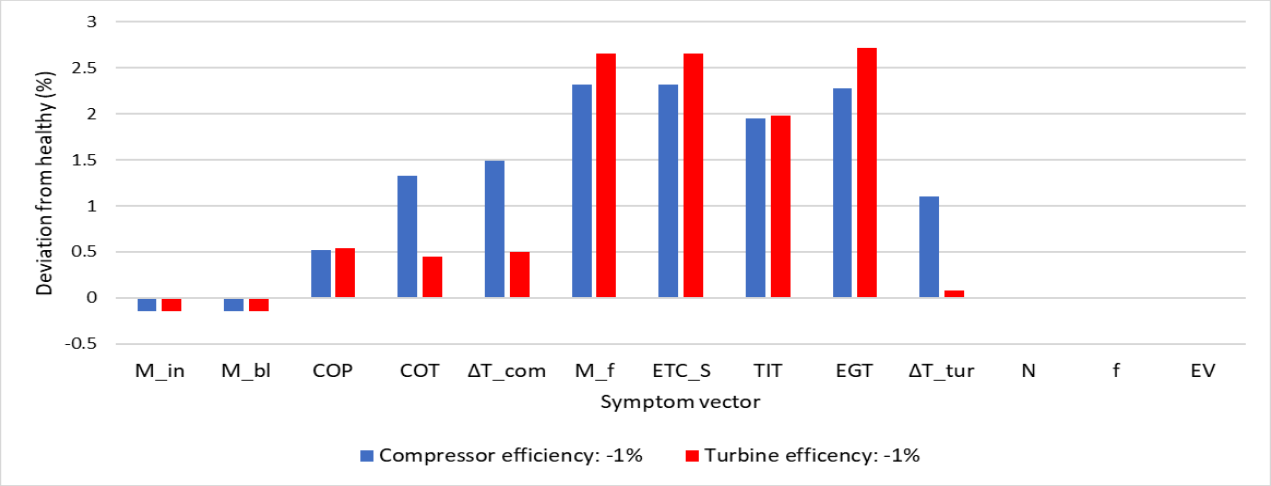


Figure 6 Comparison of the compressor and turbine faults

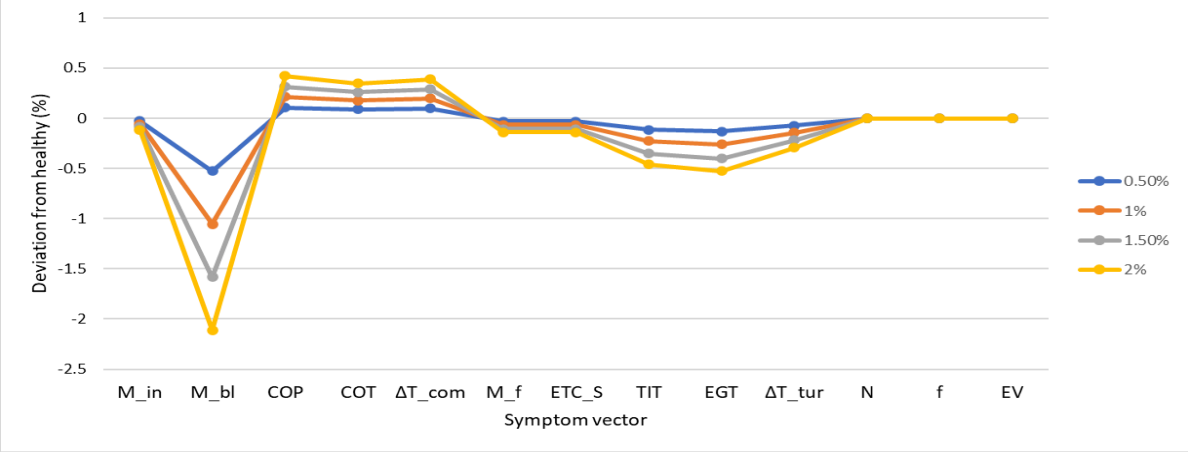
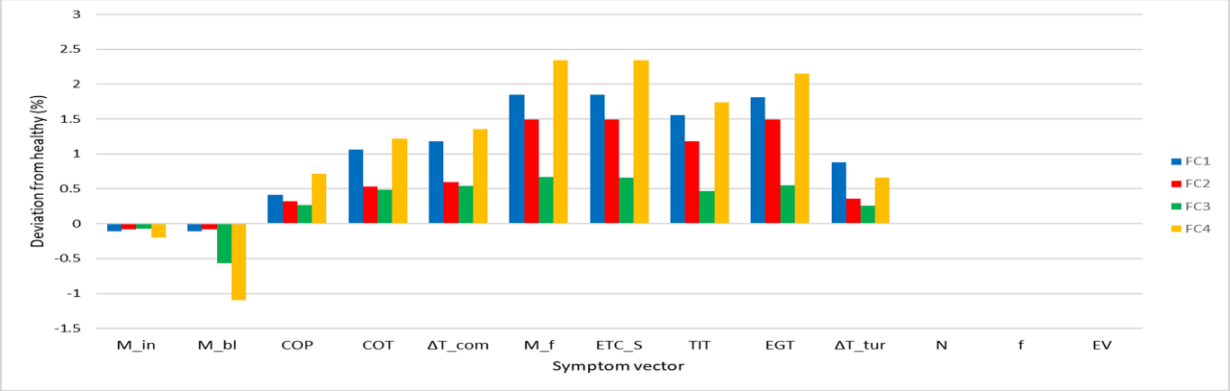


Figure 7 Sensitivity assessment for the LCV fault

Following the compressor and turbine faults, the effect of a sticking valve on the APU performance is investigated. Under this fault, the valve is assumed to get stuck at a position that results in reduced bleed flow compared to the operator's demand, and for this reason, the sticking valve fault is emulated by decreasing the bleed flow demand. Figure 7 presents the changes in the symptom vector due to the LCV's fault for various severity levels and Figure 3 (N3) illustrates the change of the compressor's operating point for reduced bleed flow by 1%. The sticking valve fault decreases the effective area at the compressor outlet, and this results in an increase in the pressure ratio and compressor outlet temperature. Based on the characteristics of the compressor performance map (Figure 3), the increase in the pressure ratio accompanies a decrease in the inlet mass flow. Since the reduction in bleed flow is more than the decrease of the inlet mass flow (Figure 7), the mass flow through the turbine increases and this results in a rise in turbine power. This phenomenon creates a tendency of the APU to increase its rotational speed and because the controller keeps the rotational speed constant, the fuel flow reduces.

Having concluded the investigation of the individual gas turbine faults, the effect of multiple faults in the APU performance are now discussed. By observing Figures 4, 5 and 7 it is noticed that the component faults discussed above have distinct features (i.e. shape of symptom vector) and can be easily identified under a single fault hypothesis. However, if multiple faults exist in the system, various fault combinations result in similar changes in the APU performance. Figure 8 illustrates an example of 4 different fault combinations that create similar changes in the symptom vector. These examples consider faults only in the gas turbine components and FC1-FC4 indicate their corresponding Fault Conditions. It can be seen that a fault diagnostic approach that is based on the single fault hypothesis will fail to identify the component health state in these cases since different fault combinations can result in similar fault patterns. The diagnostic technique that is proposed in this work takes into account cases where multiple faults exist in the system and the diagnostic classifiers are trained accordingly. The strengths and weaknesses of the proposed technique are discussed in Section 5.



	Compressor efficiency decrease	Turbine efficiency decrease	Bleed flow decrease	SS signal bias	FMV position stuck increased from healthy state	Generator stator resistance increased
FC1	0.8%	0%	0%	0%	0%	0%
FC2	0.3%	0.3%	0%	0%	0%	0%
FC3	0.3%	0%	0.5%	0%	0%	0%
FC4	0.7%	0.3%	0.9%	0%	0%	0%

Figure 8 Gas turbine multiple fault combinations

4.2. Control & fuel system faults

Following the gas turbine components, faults in the control and fuel system are analysed. In this section, fault modes for steady-state operation are considered for the Speed Sensor (SS) and the Fuel Metering Valve (FMV).

As regards the SS, the simulated fault emulates a condition under which the rotational speed signal that is transferred to the APU Electronic Turbine Controller (ETC) has a constant positive bias, i.e. the actual speed is lower than that indicated. Figure 9 presents the corresponding changes in the symptom vector and Figure 3 (N4) illustrates the compressor operating point that corresponds to a 0.5% biased signal. This fault makes the controller reduce the fuel flow in order to decrease the rotational speed until the difference between the sensed rotational speed and the APU's design rotational speed (20,000 rpm) drop below a predefined threshold. This threshold sets the convergence limit of the PI controller that is used to emulate the ETC. For this reason, the change of the rotational speed under the SS fault does not match exactly with the bias injected in the SS. Under this fault, the compressor operating point moves to a lower speed line, which corresponds to a reduced inlet mass flow and pressure ratio (Figures 3 and 9). Finally, the reduced rotational speed decreases the generator's

frequency, and this drives the generator's controller to increase the excitation voltage to maintain a constant output voltage.

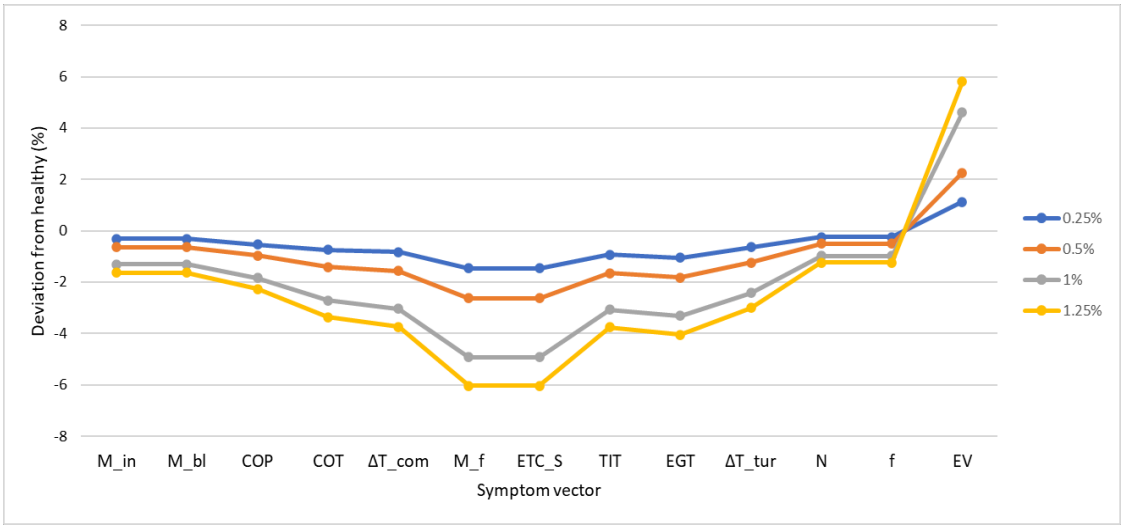


Figure 9 Sensitivity assessment for the speed sensor fault

The FMV fault replicates a sticking valve condition that keeps the fuel flow constant regardless of the controller's command. Figure 10 presents the changes in the symptom vector for the FMV fault, and Figure 3 (N5) illustrates the compressor operating point for a stuck FMV in a position that increases the fuel flow by 1% compared to the healthy state. Under this fault, since the fuel flow remains constant, the turbine power increases, and this leads to an increase in the rotational speed. The controller senses the over-speed condition and commands the FMV to close. Since the FMV does not react to the control signals, the controller dictates the FMV to become fully closed and this explains the huge difference that is observed to the "ETC_signal" parameter (Figure 10). The controller's behaviour is related to the fact that the FMV ignores the control signal, therefore, regardless of the fault's severity, the controller will always command the FMV to become fully close. Furthermore, the increased rotational speed drives the compressor operating point to a higher speed line that very slightly decreases the mass flow and increases the pressure ratio, as shown in Figure 3. Finally, the rise in the rotational speed increases the generator's frequency, which decreases the excitation voltage.

The effects of the SS and FMV faults on the APU performance, like the gas turbine faults, are distinct and can be easily identified under single fault modes. However, when multiple faults exist in the

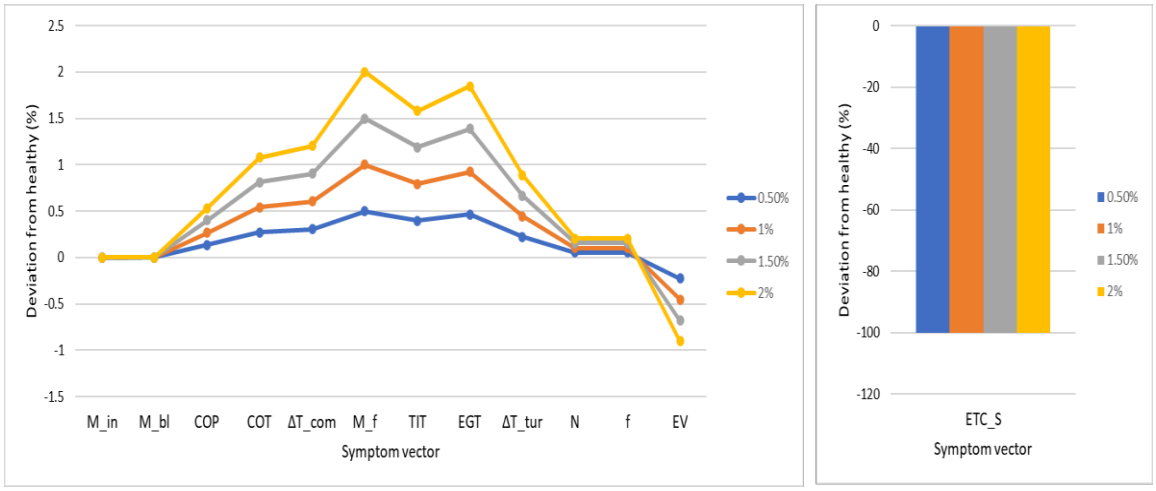
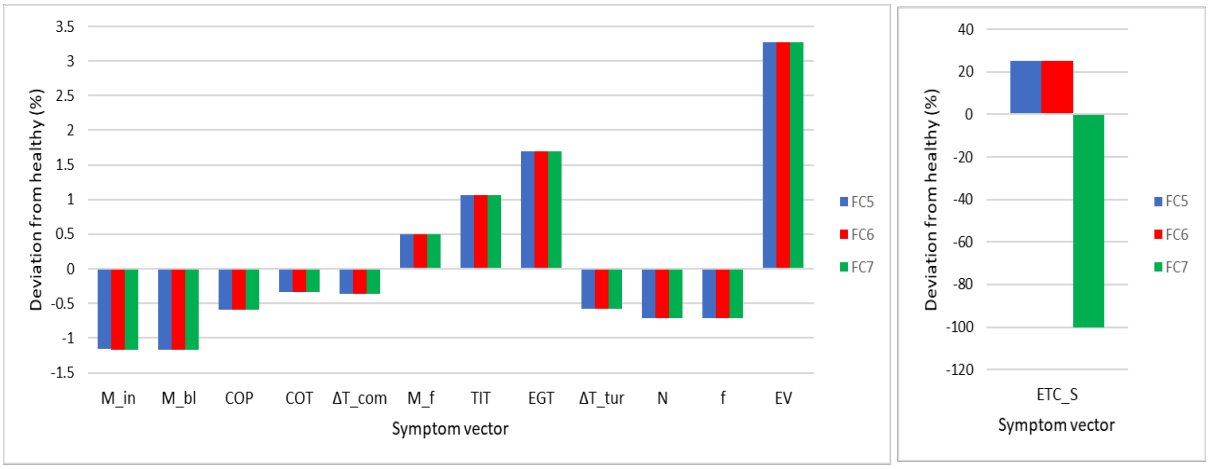


Figure 10 Sensitivity assessment for the FMV fault



	Compressor efficiency decrease	Turbine efficiency decrease	Bleed flow decrease	SS signal bias	FMV position stuck increased from healthy state	Generator stator resistance increased
FC5	1%	1%	0%	0%	0.5%	0%
FC6	1%	1%	0%	0.2%	0.5%	0%
FC7	1%	1%	0%	0.8%	0.5%	0%

Figure 11 Fault combination that can mask the SS fault

system, the imposed changes on the symptom vector can vary and sometimes a fault can be completely masked. These situations are presented in the examples FC5-FC7 that are illustrated in Figure 11. Initially, the test case FC5 (Figure 11) is considered. In this test case, the compressor and turbine efficiencies are decreased by 1%, and the FMV is stuck in a position that allows 0.5% more fuel flow compared to the healthy state. Under this fault combination, the constant fuel flow is not enough to drive the gas turbine's rotational speed up to its rated value, due to the compressor and turbine degradation. The controller senses an under-speed condition and commands the FMV to open. This example demonstrates that the FMV fault can result in over-speed or under-speed conditions depending on the health state of the other components.

The example FC6 considers a test case that includes the faults described in FC5 supplemented with a fault in the SS. It is observed that the changes imposed on the symptom vector for FC6 are identical with the changes that correspond to FC5, hence the SS fault is completely masked. This occurs because, as it was explained above, the faults in FC5 create an under-speed condition and the severity of the SS fault in FC6 is not strong enough to stimulate an over-speed. Therefore, the addition of a SS fault with low severity to FC5 does not affect the symptom vector, because the fuel flow remains constant (the FMV is stuck) and the controller's command corresponds to an under-speed condition. In a test case that the SS fault severity is strong enough to create an over-speed condition, as seen in the example in FC7, the controller commands the opposite reaction compared to the previous test cases, hence the SS fault can be identified.

4.3. Generator fault

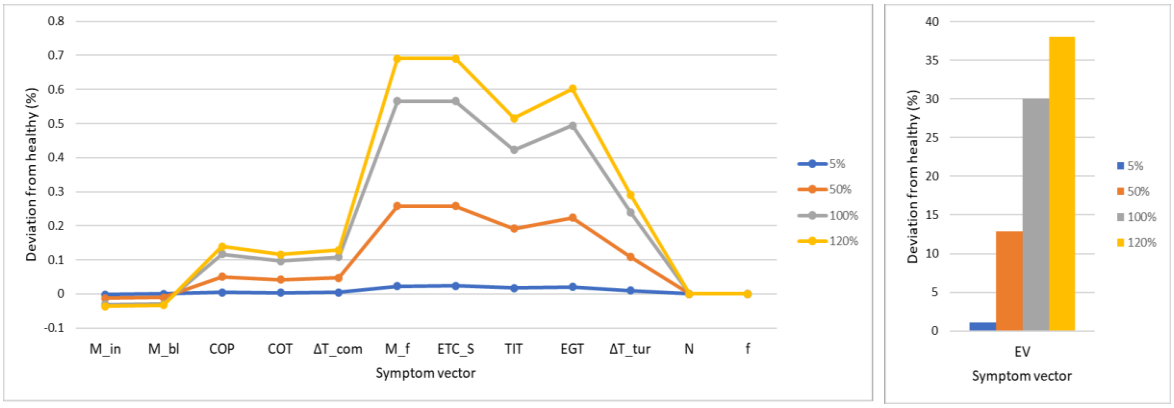


Figure 12 Sensitivity assessment for the generator

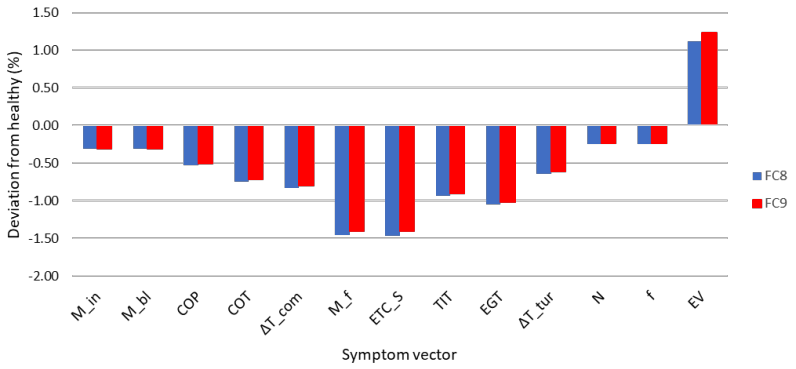
The failure modes that can be developed in an electric generator are numerous and can affect both the electrical part and the mechanical part of the generator. For this work, a simple electrical fault that simulates the increase in the stator's resistance is considered. Under this fault, the generator's output voltage presents a tendency to decrease. The generator's controller increases the excitation voltage (EV), which generates a magnetic flux to keep the output voltage constant. The increased EV results in an increase in the armature voltage, which in turn leads to an increase in power demanded from the gas turbine's shaft.

Figure 12 presents the changes imposed on the symptom vector under the generator fault, corresponding to 4 different levels of degradation. It is observed that the influence of the generator fault on the gas turbine parameters increases as the stator resistance rises. However, the changes remain small even when the fault severity increases by 120%. This phenomenon is associated with the fact that the change in the electrical power demand due to the generator fault is very minor compared with the pneumatic power extracted, 7-8% from Table 3.

Table 3 Comparison of the generator power with the pneumatic power

	Pneumatic Power (kW)	Generator power imposed on the gas turbine's shaft (kW)	$\frac{P_{gen}}{P_{bl}}$	Deviation from healthy (%)
Healthy	533.54	35.53	0.07	0.00
Fault: 5%	535.28	35.72	0.07	0.19
Fault: 50%	533.74	37.42	0.07	5.28
Fault: 100%	533.96	39.65	0.07	11.50
Fault: 120%	534.07	40.59	0.08	14.13

The test case that corresponds to an increase in the stator resistance by 120% is used as a working example and, based on that, it can be observed that the increase from healthy by 14.13% leads to minor changes in the gas turbine characteristics. More specifically, the maximum change is observed in the fuel flow and the minimum change in the inlet mass flow. The only parameter that has a significant reaction under the generator fault is the excitation voltage, which increases by 38%. The excitation voltage is adjusted by the generator's controller and depends only on the gas turbine rotational speed and the generator's health state. Fault combinations that result in changes in the rotational speed affect the excitation voltage. Therefore, under such conditions, the generator's health state can be misclassified. Figure 13 presents an example of two fault combinations that have similar fault patterns. For FC8 the generator is healthy, and for FC9 the generator's internal resistance is increased by 3%. It is observed that both fault modes cause almost identical changes in the symptom vector. These phenomena create ambiguities in the generator's diagnosis. This will be discussed more thoroughly in Section 5.



	Compressor efficiency decrease	Turbine efficiency decrease	Bleed flow decrease	SS signal bias	FMV position stuck increased from healthy state	Generator stator resistance increase
FC8	0%	0%	0%	0%	0.25%	0%
FC9	0%	0%	0%	0%	0.24%	1%

Figure 13 Fault combinations that result in ambiguity in the generator fault diagnosis

4.4. Definition of the degradation range for components considered in the diagnostic analysis

The definition of the degradation range for each component that will be considered in the diagnostic analysis is driven by two major factors: the safety-critical parameters must remain within their limits, and the injected faults should impose changes on the symptom vector parameters that are of the same order of magnitude.

As regards the analysis that is considered in this paper, the relevant safety parameters are the Exhaust Gas Temperature (EGT), which must be below 620 °C, and the rotational speed, which must be between 19,000 rpm and 21,000 rpm. The faults that increase the EGT are the compressor, turbine, FMV and generator. Based on the sensitivity assessment of these faults, the EGT reaches its maximum value when the compressor, the turbine and the generator are degraded.

The fault severity that is selected for these components, in order to keep the EGT within its limit, is 1% decrease in the efficiency of the compressor and turbine and 5% increase in the generator's stator resistance. As regards the LCV, SS and FMV faults, their degradation ranges are selected in such a way that their influence on the symptom vector is of the same order of magnitude compared with the components mentioned above. Therefore their fault severity is selected to be: 1% reduced bleed flow for the LCV, 0.5% bias for the SS and 1% increased position for the FMV.

5. Diagnostic analysis

The ultimate aim of this project is to develop a diagnostic technique that can diagnose APU component faults. The diagnostic technique that is proposed in this paper uses a classification algorithm to identify each component's health state (healthy or faulty). As has been discussed in Section 4, the diagnosis of component health state under multiple faults is a challenging task, because many times different component faults result in similar fault patterns, even if the correct sensor signals are chosen for the symptom vector. The diagnostic technique that is proposed in this work aims to train diagnostic classifiers to recognise component health state under single or multiple faults.

In order to achieve this, instead of training each classifier under the single fault hypothesis, a training strategy that considers 4 different scenarios regarding the system health state (Table 2) is used. The fault scenarios that are considered, apart from the single fault hypothesis (Scenario 1), are the simultaneous existence of multiple components faults (Scenarios 2 and 3), and the possibility that all components have a level of degradation (Scenario 4). Thus, each classifier is trained to recognise the health state of the component under investigation while the other components can be healthy or have various fault combinations. Therefore, each classifier is able to identify unique fault features for each component fault and this allows the diagnosis of different faults that impose similar changes to the APU performance.

Data for training and testing the diagnostic classifiers are generated from the Boeing 747 APU model that has been discussed throughout this paper, and the corresponding boundary conditions that are presented in Section 4. The simulation data are then processed by supervised classification algorithms that are included in the Matlab classification learner toolbox [35]. The algorithms that are included in Matlab are well-known classifiers (e.g. Support Vector Machine, k-nearest neighbour) and for this reason, their mathematical description is not provided in this paper. For each component under investigation, the simulation data that corresponds to the four scenarios of Table 1 is used to train all available classifiers, and the one that demonstrated the best classification results is selected. The classifier that is chosen for each component is shown in Table 2.

Training of each classification algorithm is conducted by considering the different system health scenarios in Table 1. 100 different simulation cases of each scenario are used to train the classifiers (4x2 scenarios from Table 1, 800 simulations in total). The component degradation severity for each simulation is randomly selected from the degradation range that is presented in Table 2. For Scenario 2, 20 faulty test cases are considered for each component (20x5 components, 100 cases in total). Finally, the component health state under Scenario 3 can be either healthy or faulty, with equal probability, for each simulation case.

The proposed methodology is tested against data corresponding to single and multiple faults for the 4 different Test Scenarios that are extracted from Table 1, as described below:

- Test Scenario 1 – Datasets that correspond to single faults for each component - 25 test cases for each component fault, 25 (test cases) x 6 (components) = 150 (total test cases), Figure 14.
- Test Scenario 2 – Datasets under which some components are healthy, while others are faulty - 25 test cases randomly generated, Figure 15.
- Test Scenario 3 – Datasets in which all components are faulty - 25 test cases randomly generated, Figure 16.
- Test Scenario 4 – Datasets in which only one component is healthy while all other components are faulty - 25 test cases for each component, 25 (test cases) x 6 (components) = 150 (total test cases), Figure 17.

The datasets that correspond to Test Scenarios 1-4 have been generated independently from the datasets that are used for training. The diagnostic results, for each component, are presented in the confusion matrices in Figures 14-17 that compare the simulated health state (vertical axis) with the classifiers' predictions (horizontal axis). For example, the symbol “GEN-H” corresponds to the generator being healthy and “GEN-F” corresponds to the generator being faulty; Figure 14d shows that a healthy generator has been classified correctly 18 times but misdiagnosed (as faulty) 7 times. Correct classification cases are positioned on the matrix diagonal and are shown in green. The false positives (cases diagnosed as faulty but actually healthy) and false negatives (diagnosed as healthy but actually faulty) are shown in rose and blue, respectively. To complete the table, the test cases that have an increased number of misclassifications are highlighted in yellow and are discussed in the rest of this section.

5.1. Test Scenario 1: single fault cases

The ability of the proposed method to detect single faults by running Test Scenario 1 is presented in Figure 14. Each matrix (a-f) shows the result of a single fault being classified by each individual classifier. A perfect result would be that all the classifiers showed their components as healthy, except the one fault that was being examined, which would classify all 25 cases as faulty. The results show that the compressor, LCV, SS and FMV classifiers have perfect accuracy, while the turbine has 2 false negatives (Figure 14b). The generator classifier presents false alarms when the SS or the FMV is faulty (Figures 14d, e).

The misclassifications for the turbine are attributed to the fact that the existence of multiple faults in the gas turbine components (compressor, turbine, and LCV) result in similar fault patterns, as it was shown in Section 4.1 (Figure 8). Therefore under specific fault combinations, the gas turbine component classifiers can result in erroneous classifications. However, the diagnostic results show that, in most test cases, the compressor, turbine, and LCV classifiers can distinguish unique fault features that correspond to each component fault and can accurately diagnose the components health state under single faults. The ability of the proposed method to identify the health state of

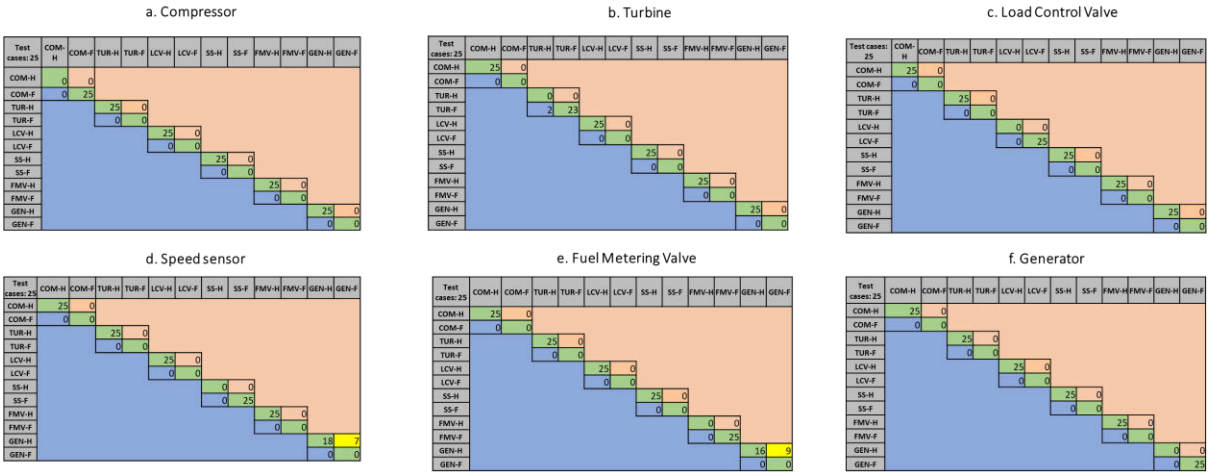


Figure 14 Diagnostic results for single faults

these components, even though their faults cause similar changes to the symptom vector, relies on the training strategy that takes into account the existence of multiple faults in the system.

As regards the SS classification results, a fault in the speed sensor results in a reduction in the rotational speed and, as seen in Section 4.2, this is a fault characteristic that corresponds only to the SS, hence the perfect classification. The perfect accuracy of the FMV fault is related to the fact that under this fault the control signal has a huge deviation compared to the healthy case, as seen in the sensitivity assessment (Section 4.2), and this is a unique fault characteristic for the FMV fault. As is also discussed in Section 4.2, the high deviation of the controller signal under the FMV fault is independent of the fault severity and appears for single or multiple fault cases. Thus, due to this fault characteristic, the FMV health state can be easily identified.

The generator health state is mostly diagnosed correctly but fails for test cases that correspond to SS or FMV faults (Figures 14d and e). As discussed in Section 4.3 the generator fault only imposes a noticeable change on the Excitation Voltage (EV), its influence on all other performance parameters being small. The EV is regulated by the generator's control unit to maintain constant output voltage, and its value depends on the generator's frequency and the armature voltage (Section 3.4, Equations 1-3). As a consequence, fault conditions that result in changes to the generator's frequency, even if the generator is healthy, will cause changes to the EV. Both the SS and the FMV faults change the generator frequency and so can be confused with a genuine generator fault. Put another way, Figure 9 shows a single SS fault, and Figure 12 a single generator fault. In the case of both the SS and generator being faulty, one of the training data scenarios which may have been labelled as a generator fault, then it is very difficult to tell the difference between this type of generator fault and a single SS fault of a higher degradation level. The same reasoning follows for the FMV case. This is a direct result of the training method chosen. If training had been performed only on single fault data, then the classifiers would have identified each fault without error.

5.2. Test Scenario 2: components either healthy or faulty

The diagnostic classifiers are next tested against datasets that correspond to multiple faults; Figure 15 presents the diagnostic results that correspond to Test Scenario 2. Under this testing scenario, there are 25 test cases in which all components could be either healthy or faulty with equal probability. Out of the 150 conditions (25x6 components), the generated cases correspond to 84 healthy components and 66 faulty ones.

Test cases: 25	COM-H	COM-F	TUR-H	TUR-F	LCV-H	LCV-F	SS-H	SS-F	FMV-H	FMV-F	GEN-H	GEN-F
COM-H	16	0										
COM-F	1	8										
TUR-H			15	0								
TUR-F			1	9								
LCV-H					12	0						
LCV-F					0	13						
SS-H							10	3				
SS-F							0	12				
FMV-H									14	0		
FMV-F									0	11		
GEN-H											7	7
GEN-F											6	5

Figure 15 Diagnostic results for multiple faults

The results in Figure 15 show that the compressor and turbine both have 1 false negative, while the LCV and FMV classifiers have perfect diagnostic accuracy. The good diagnostic results for the gas turbine components under multiple faults is attributed to the training strategy that considers multiple fault combinations. The misclassifications that are observed are associated with the fact that these gas turbine faults can sometimes impose very similar changes on the APU performance, as explained in Section 4.1.

The SS and generator classifiers demonstrate lower accuracy. The SS classifier has 3 false positives, but no false negatives, showing that the SS classifier can recognise a fault, but can also result in false positives under specific fault conditions. These cases correspond to those in which the compressor, turbine and FMV are faulty. As was seen in Section 4.2, in such cases, if the SS fault severity is low, the changes in the SS health state do not markedly affect the symptom vector. As a consequence, the SS classifier is not able to recognise characteristic features in the symptom vector that correspond to the SS healthy or faulty state, and hence the classifier fails.

The generator classifier has 7 false positives and 6 false negatives, hence its diagnostic results are not reliable. The unsuccessful diagnostic results for the generator's classifier are related to the fact that the changes that the generator fault imposes on the gas turbine performance are negligible and any major fault is characterised by a change in EV. Therefore, SS or FMV faults that also change the EV can cause misclassification in the generator diagnosis, as it was explained in Section 5.1.

5.3. Test Scenario 3: all components faulty

Test cases: 25	COM-H	COM-F	TUR-H	TUR-F	LCV-H	LCV-F	SS-H	SS-F	FMV-H	FMV-F	GEN-H	GEN-F
COM-H	0	0										
COM-F	1	24										
TUR-H			0	0								
TUR-F			3	22								
LCV-H					0	0						
LCV-F					0	25						
SS-H							0	0				
SS-F							0	25				
FMV-H									0	0		
FMV-F									0	25		
GEN-H											0	0
GEN-F											10	15

Figure 16 Diagnostic results when all components are degraded

Identification of component faults when all components are degraded, Test Scenario 3, is investigated here. The diagnostic results presented in Figure 16 show that a fault can be detected, with good accuracy, in all components apart from the generator.

More specifically, the LCV, SS and FMV have perfect fault detection accuracy, and there exists only a few false negatives for the compressor (1) and for the turbine (3). As previously discussed, the fault misclassifications for the compressor and the turbine are associated with the fact that faults in the gas

turbine components result in similar changes in the APU performance. In most test cases the classifiers have accurate classification results, and this (once again) highlights the merits of the training strategy that considers multiple component faults. The unique characteristics of the SS and FMV faults, discussed in Section 5.1, are again recognised by their respective classifiers.

The generator classifier has, again, low fault detection accuracy since it has 10 false negatives, and hence the generator predictions are not trustworthy. The generator classifier fails to identify the generator's health state for the same reason that the generator diagnosis fails in Test Scenarios 1 and 2.

5.4. Test Scenario 4: one component healthy, all others faulty

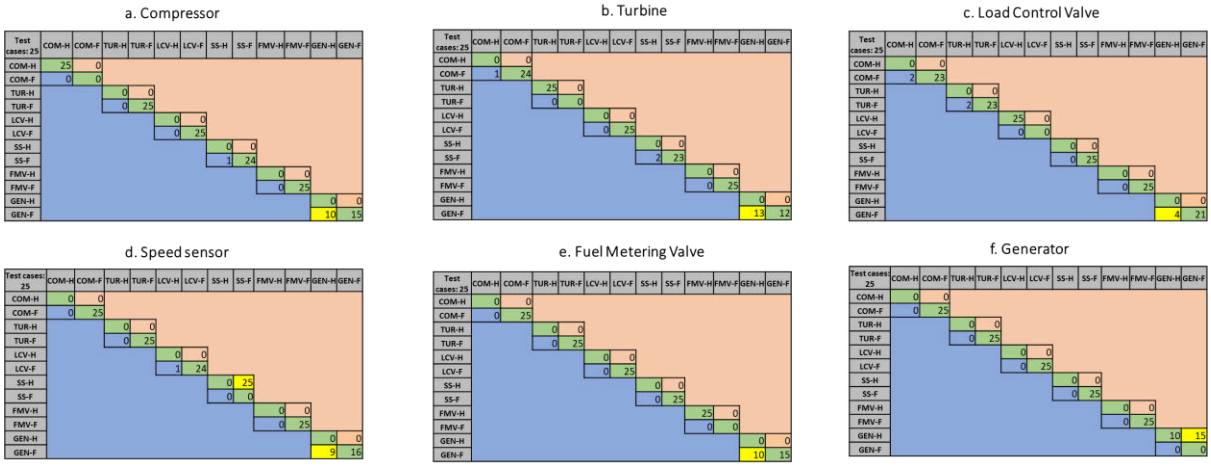


Figure 17 Diagnostic results when one component healthy, all others faulty

Finally, the ability of the proposed method to identify a healthy component when all other components are degraded (Test Scenario 4) is presented in Figure 17. The results show that the classifiers that correspond to the compressor, turbine, LCV and FMV, can diagnose their component's health state with good accuracy, while the SS and generator classifiers do not provide accurate predictions. Indeed the FMV has perfect classification accuracy.

The maximum number of false negatives for the compressor, turbine, and LCV are:

- 2 each for the compressor and turbine, which correspond to the test condition where all components, apart from the LCV, are degraded (Figure 17c).
- 1 for the LCV, which corresponds to the test condition where all components are degraded apart from the SS (Figure 17d).

As has been pointed out in all the previous tests, due to the training strategy that trains the classifiers to consider the existence of multiple faults in the system, the compressor, turbine and LCV classifiers can diagnose the component's health state with a high level of accuracy for single and multiple fault conditions, even though their fault patterns are very similar. As such, the above results are seen as good.

The SS classifier cannot recognise the SS healthy state when all other components are degraded and the classification results in false alarms for all test cases (Figure 17 d). Under these test cases, the compressor, turbine and FMV are simultaneously degraded and, as was discussed in Section 5.2, in

such cases the SS fault does not markedly influence the symptom vector. This situation does not allow the SS classifier to differentiate between healthy or faulty cases.

Finally, the generator's classifier, similarly to all the previous tests, cannot predict the generator's health state since it presents many false positives and negatives. The reason that the generator diagnosis fails when multiple faults are simultaneously degraded are the same as in the previous tests.

5.5. Diagnostic Summary

The major findings from the diagnostics can be summarised as:

- The compressor, turbine, LCV and FMV have good classification accuracy. This is perhaps surprising as their individual degraded health results in similar changes in APU performance.
- The SS and generator classifiers do not provide reliable predictions.
- The symptom vector for these studies was chosen by engineering judgement. It could now be refined, or alternative sensors suggested, in light of these results.
- For the SS, a secondary speed sensor could be installed (redundancy) to alleviate this fault.
- For the generator, as this component is effectively de-coupled from the main gas turbine, the system diagnosis approach could be complemented with a component diagnostic approach. A sensor that provides measurement of the resistance of the generator windings can detect a fault in this component.
- The overall strategy, of training the classifiers on data sets with a mixture of faults, seems to indicate a promising way forward. In particular, the results shown as Test Scenarios 2 and 3 represent cases found in industry. The condition of a component is being examined without knowing the condition of the components around it.

Summary and conclusions

In this paper the simulation of faults in selected components of a Boeing 747 APU is presented, and a diagnostic technique that aims to identify the health state of these components under single or multiple faults reported. The selection of the APU components is based on the most frequent component faults that have been reported by The Boeing Company and the fault mode that is simulated for each component is driven by the relevant studies in the public domain literature that discuss the component degradation mechanisms.

The aim of this work is to conduct a system level diagnostic analysis on an APU and is based on two important aspects:

- The analysis considers component faults of multiple sub-systems.
- The proposed diagnostic technique is designed to identify single and multiple faults.

Both aspects that are mentioned above, have not been sufficiently discussed by relevant studies in the public domain literature, thus, the analysis and the findings that are reported in this paper contribute to this issue.

The diagnostic technique that is proposed in this paper is able to diagnose the compressor, turbine, LCV, and FMV health state, under single and multiple faults. These faults result in similar fault patterns, and the ability of the proposed technique to identify the components health state suggests a promising way forward. The outcome of the diagnostic analysis, indicates that the training of the component classifiers by considering the simultaneous existence of faults in different components is critical in the diagnosis of single and multiple faults. Also, the reasons that the SS and generator

diagnosis fail are explained and based on this discussion, there are suggested ways to enhance the diagnostic results.

Finally, the results of this work suggest interesting topics that can be investigated in order to increase the system diagnostic capability. For instance, the influence of sensor noise on the symptom vector parameters would impose a further limitation on the component diagnostic. Then the ability of the diagnostic technique to distinguish between the sensors uncertainty and the existence of component faults would be a challenging task. Also, this would set more realistic thresholds to the fault severity range. Another topic that is worthy of studying is the identification of the minimum number of sensors required to diagnose the maximum number of component faults. The answer to this question would suggest design specifications for systems that are built for fault diagnostics.

Nomenclature

Abbreviations

APU	Auxiliary Power Unit
AVR	Automatic Voltage Regulator
COP	Compressor Outlet Pressure
COT	Compressor Outlet Temperature
DLM	Dynamic Linear Model
EGT	Exhaust Gas Temperature
ETC	Electronic Turbine Controller
EV	Excitation Voltage
FADEC	Full Authority Digital Electronic
FC	Fault Condition
FMV	Fuel Metering Valve
LCV	Load Control Valve
LRU	Line Replaceable Unit
ML	Machine Learning
RUL	Remaining Useful Life
SS	Speed Sensor
TD	Test Datasets
TIT	Turbine Inlet Temperature

Latin symbols

$()_{com}$	A quantity that corresponds to the compressor
$()_{tur}$	A quantity that corresponds to the turbine
$C_{p,air}$	Air specific heat at constant pressure
$C_{p,gas}$	Gas specific heat at constant pressure
I_{load}	Generator current output
$\dot{m}_{bl}$	Bleed flow
$\dot{m}_{f}$	Fuel flow
$\dot{m}_{in}$	Inlet mass flow
N_{gen}	Generator rotational speed
P_{com}	Compressor power
P_{tur}	Turbine power
P_{bl}	Bleed air power
P_{gen}	Generator power demand
R_{arm}	Generator armature resistance
R_{stat}	Generator stator resistance
V_{arm}	Generator armature voltage

V_{ex}	Generator excitation voltage
V_{out}	Generator output voltage
X_{in}	Generator windings inductive reactance

Greek symbols

ΔT	Temperature difference
η_{com_isen}	Compressor isentropic efficiency
η_{tur_isen}	Turbine isentropic efficiency
φ	Generator internal magnetic flux

Acknowledgements

The authors would like to thank and acknowledge The Boeing Company for funding and supporting the project.

References

[1] X. Liu, L. Liu, L. Wang, Q. Guo, and X. Peng, 2019, "Performance sensing data prediction for an aircraft auxiliary power unit using the optimized extreme learning machine" *Sensors*, vol. 19, no. 18.

[2] A. Yabsley and Y. Ibrahim, 2008, "Study on maintenance contribution to life cycle costs: Aircraft auxiliary power unit example" in *Proceedings of the IEEE International Conference on Industrial Technology*, Chengdu, China.

[3] C. Skliros, A. Fakhre, and I. Jennions, 2020, "Fault Simulations and Diagnostics for a Boeing 747 Auxiliary Power Unit" *J. Eng. Gas Turbine Power*, (accepted for publication June 2020).

[4] T. Siebel, J. Zanger, A. Huber, M. Aigner, K. Knobloch, and F. Bake, 2018, "Experimental investigation of cycle properties, noise, and air pollutant emissions of an APS3200 auxiliary power unit," *J. Eng. Gas Turbines Power*, vol. 140, no. 6, pp. 1–9.

[5] D. Gorinevsky, E. Nwadiogbu, and D. Mylaraswamyt, 2002, "Model-based Diagnostics for Small-scale Turbomachines," in *Conference of Decision and Control*, Las Vegas, Nevada.

[6] D. Gorinevsky, K. Dittmar, D. Mylaraswamy, and E. Nwadiogbu, 2002, "Model-Based Diagnostics for an Aircraft Auxiliary Power Unit," *IEEE International Conference on Control Applications*. Glasgow, Scotland.

[7] Y. Lei, B. Yang, X. Jiang, F. Jia, N. Li, and A. K. Nandi, 2020, "Applications of machine learning to machine fault diagnosis : A review and roadmap," *Mech. Syst. Signal Process.*, vol. 138.

[8] W. O. L. Vianna, J. P. P. Gomes, R. K. H. Galvão, T. Yoneyama, and J. P. Matsuura, 2014, "Health monitoring of an auxiliary power unit using a classification tree," *Proc. Annu. Conf. Progn. Heal. Manag. Soc. 2011, Montreal, Canada*.

[9] R. M. Pascoal, W. O. L. L. Vianna, J. P. P. P. Gomes, and R. K. H. H. Galvão, 2013, "Estimation of APU failure parameters employing linear regression and neural networks," *PHM 2013 - Proc. Annu. Conf. Progn. Heal. Manag. Soc. 2013*, New Orleans, LA.

[10] F. Wang, J. Sun, X. Liu, and C. Liu, 2019, "Aircraft auxiliary power unit performance assessment and remaining useful life evaluation for predictive maintenance," *Proc. Inst. Mech. Eng. Part A J. Power Energy*, pp. 1–13.

[11] C. Skliros, M. Esperon Miguez, A. Fakhre, and I. Jennions, 2019, "A review of model based and data driven methods targeting hardware systems diagnostics," *Diagnostyka*, vol. 20, no. 1,

pp. 3–21.

[12] R. Kurz and K. Brun, “Degradation in gas turbine systems, 2001,” *J. Eng. Gas Turbines Power*, vol. 123, no. 1, pp. 70–77.

[13] W. Kappis, 2013, “Impact of Degradation on the Operational Behavior of a Stationary Gas Turbine and in Detail on the Associated Compressor,” in *Turbomachinery Symposium*, Doha, Qatar.

[14] P. C. Frith, 1992, “The Effect of Compressor Rotor Tip Crops,” in *International Gas Turbine and Aeroengine Congress and Exposition*, Cologne, Germany.

[15] M. B. Graf *et al.*, 1998, “Effects of non- Axisymmetric tip clearance on axial compressor performance and stability,” *J. Eng. Gas Turbines Power*, vol. 120.

[16] P. C. Frith, 1992, “The effect of compressor rotor tip crops on turboshaft engine performance,” in *International Gas Turbine Aeroengine Congress and Exposition, Cologne, Germany*.

[17] F. C. Mund and P. Pilidis, 2005, “Online compressor washing: A numerical survey of influencing parameters,” *Proc. Inst. Mech. Eng. Part A J. Power Energy*, vol. 219, no. 1, pp. 13–23.

[18] D. Fouflias *et al.*, 2010, “Experimental investigation of the influence of fouling on compressor cascade characteristics and implications for gas turbine engine performance,” *Proc. Inst. Mech. Eng. Part A J. Power Energy*, vol. 224, no. 7, pp. 1007–1018.

[19] R. J. Boyle, 1994, “Prediction of surface roughness and incidence effects on turbine performance,” Journal of Turbomachinery, vol. 116.

[20] I. S. Diakunchak, 1991, “Performance deterioration in industrial gas turbines,” *J. Eng. Gas Turbines Power*, vol. 161.

[21] L. Shang and G. Liu, 2011, “Sensor and actuator fault detection and isolation for a high performance aircraft engine bleed air temperature control system,” *IEEE Trans. Control Syst. Technol.*, vol. 19, no. 5, pp. 1260–1268, 2011.

[22] M. J. Daigle and K. Goebel, 2011, “A model-based prognostics approach applied to pneumatic valves,” *Int. J. Progn. Heal. Manag.*, vol. 2, no. 2.

[23] E. Balaban, A. Saxena, P. Bansal, K. F. Goebel, and S. Curran, 2009, “Modeling, detection, and disambiguation of sensor faults for aerospace applications,” *IEEE Sens. J.*, vol. 9, no. 12, pp. 1907–1917.

[24] K. Goebel and W. Yan, 2008, “Correcting Sensor Drift and Intermittency Faults With Data Fusion and Automated Learning,” *IEEE Syst. J.*, vol. 2, no. 2, pp. 189–197.

[25] L. Xiao, Z. Meng, X. Huang, and L. Ma, 2019, “Adaptive observer based fault tolerant control for aircraft engine with sensors and actuators faults,” *Chinese Control Conf. CCC*, Guangzhou, China.

[26] E. Balaban, A. Saxena, P. Bansal, K. F. Goebel, P. Stoelting, and S. Curran, 2009, “A diagnostic approach for electro-mechanical actuators in aerospace systems,” *IEEE Aerosp. Conf. Proc.*, Big Sky, MT.

[27] Y. Cao, J. Wang, R. Xie, and X. Wang, 2015, “Fault tree analysis of electro-mechanical actuators,” *Chinese Control Conf. CCC*, Hangzhou, China.

[28] T. D. Batzel, D. C. Swanson, and J. F. Defenbaugh, 2003, “Predictive diagnostics for the main field winding and rotating rectifier assembly in the brushless synchronous generator,” *IEEE Int. Symp. Diagnostics Electr. Mach. Power Electron. Drives, SDEMPED 2003, Atlanta, GA*.

[29] T. D. Batzel and D. C. Swanson, 2009, “Prognostic health management of aircraft power generators,” *IEEE Trans. Aerosp. Electron. Syst.*, vol. 45, no. 2, pp. 473–483, 2009.

[30] A. Tantawy, X. Koutsoukos, and G. Biswas, 2012, “Aircraft power generators: Hybrid modeling and simulation for fault detection,” *IEEE Trans. Aerosp. Electron. Syst.*, vol. 48, no. 1, pp. 552–571.

[31] R. Bettocchi, M. Pinelli, P. R. Spina, and M. Venturini, 2007, “Artificial intelligence for the diagnostics of gas turbines - Part II: Neuro-fuzzy approach,” *J. Eng. Gas Turbines Power*, vol. 129.

[32] R. Bettocchi, M. Pinelli, P. R. Spina, and M. Venturini, 2007, “Artificial intelligence for the diagnostics of gas turbines - Part I: Neural network approach,” *J. Eng. Gas Turbines Power*, vol. 129.

[33] Hare, J., Gupta, S., Najjar, N., D'Orlando, P. et al., 2015, "System-Level Fault Diagnosis with Application to the Environmental Control System of an Aircraft," SAE Technical Paper 2015-01-2583, 2015, doi:10.4271/2015-01-2583.

[34] J. Norton, 2015, “An introduction to sensitivity assessment of simulation models,” *Environ. Model. Softw.*, vol. 69, pp. 166–174.

[35] MathWorks, “Classification Learner Documentation”, accessed at June 24, 2020, https://www.mathworks.com/help/stats/classificationlearner-app.html.



https://dspace.org/

Fault simulations and diagnostics for a Boeing 747 Auxiliary Power Unit

Skliros, Christos; Ali, Fakhre; Jennions, Ian

2021-07-01
Elsevier
https://doi.org/10.1016/j.eswa.2021.115504
Skliros C, Ali F, Jennions I. (2021) Fault simulations and diagnostics for a Boeing 747 Auxiliary Power Unit. Expert Systems with Applications, Volume 184, December 2021, Article number 115504

Downloaded from a DSpace repository. https://dspace.org/